Hindawi
Advances in Civil Engineering
Volume 2020, Article ID 9708327, 13 pages
https://doi.org/10.1155/2020/9708327

Research Article

Experimental Study on the System Performance of Adjacent Precast Concrete Box Beam Bridges

Yanling Leng,[1] **Jinquan Zhang**,[2] **Ruinian Jiang**,[3] **and Yangjian Xiao**[4]

[1]*IMEG Corp., Sioux Falls, SD, USA*
[2]*Chongqing Jiaotong University, Chongqing, China*
[3]*Department of Engineering Technology & Surveying Engineering, New Mexico State University, Las Cruces, NM, USA*
[4]*Department of Civil Engineering, Chongqing Jiaotong University, Chongqing, China*

Correspondence should be addressed to Ruinian Jiang; rjiang@nmsu.edu

Received 11 October 2019; Revised 30 January 2020; Accepted 12 February 2020; Published 13 March 2020

Academic Editor: Luís C. Neves

Analyses of catastrophic collapse of some adjacent precast concrete box beam bridges reveal the fact that the hinge joints between the adjacent beams were not sufficiently designed. The joint failure caused by deterioration is the result of system reliability deficiency of this type of bridges. To understand the system performance of the bridges, the redundancy and robustness of a bridge model with a scale of 1 : 2, based on the prototype design drawings for 10-meter adjacent box beam bridges in China, were assessed through a system safety evaluation procedure. The result confirmed the assumption that the redundancy and robustness of certain adjacent precast concrete beam bridges did not meet the pertinent requirements proposed in National Cooperative Highway Research Program (NCHRP) reports 406, 458, and 776 as a result of hinge joint failure. To address the current design deficiencies, a system factor is recommended in this paper to calculate the nominal resistance that reflects the level of redundancy of this type of bridges. In addition, a new framework is proposed to address the particular structural feature and topology of adjacent precast concrete beam bridges for the assessment of structural redundancy and robustness, which can reduce the computation complexity compared to existing approaches. The full-range load test performed in this research verified the previous research results on bridge system safety that were mainly based on theoretical analysis and simulations.

1. Introduction

Adjacent precast concrete box beam bridges are widely used worldwide because of their unique advantages including the simple structural design, quick installation, and high cost effectiveness. The first bridge of this type was built in the United States in the 1950s; at present, about two-thirds of states in the United States have built precast adjacent box beam bridges, which account for nearly one-sixth of the bridges built annually on public roads [1]. China has approximately 170,000 adjacent box beam bridges, which account for about 25 percent of the total bridges in China [2].

The bridges are built by placing precast concrete box beams side by side in parallel. The beams are then connected using hinge joints longitudinally grouted in between (also named "shear keys") and covered with a concrete pavement deck. The hinge joints and the concrete deck provide the transverse connection between concrete box beams. Tie rods or transverse posttensioning strands may be used to further strengthen the transverse connection.

Most adjacent box beam bridges have been in service for many years and generally performed well. A recurring problem, however, is the cracking of hinge joints, normally occurring within 2 to 5 service years according to an investigation conducted by the authors in China [3], while the expected service life for concrete bridges is normally in the range between 75 and 120 years [4, 5]. The cracking of hinge joints leads to water leakage, corrosion, and even a complete loss of load transfer capacity among beams, which is called the "Single Plate Load Effect" [6–8]. Fatigue and temperature changes also contribute to the cracking of hinge joints [9].

When loads cannot transfer between adjacent beams, damage to both the structure and vehicles can be triggered on the loaded beam by heavy trucks. Figure 1 shows two such events: (a) the collapse of an exterior beam of the Lake View Drive Bridge in Washington County, PA, in 2005 and (b) the collapse of the exterior beam of the approach bridge of the 3rd Hangzhou Qiantang Bridge in China in 2010.

In 2005, the fascia beam supporting the east-side parapet wall of the third span of the Lake View Drive Bridge failed under the action of dead load. The bridge girders were in service for 42 years before the bridge collapsed. Following an extensive visual inspection, the girders were saw-cut near their failure regions to permit an extensive forensic investigation. After demolition of the bridge, asphalt was found on the lower edge of the hinge joints, confirming that the joints were no longer functional; as a result, no load was distributed transversely across the bridge, implying a girder having deteriorated hinge joints may experience live-load moments 66% greater than those expected in the design [10].

Similarly, the function loss of the edge hinge joint was the main cause of the collapse of the exterior beam of the approach bridge of the 3rd Hangzhou Qiantang Bridge. The damage of the edge hinge joint resulted in the formation of the "Single Plate Load Effect"; as a result, no load was transferred between the adjacent beams.

The load carrying capacity evaluation of adjacent precast concrete box beam bridges is presently based on elastic analysis. Lateral load distribution factors are calculated for beams, and the ultimate loading capacity of the individual beams is evaluated based on the distributed load. The system performance of the bridge is currently simply reflected by lateral load distribution factors, which are determined in the elastic range and do not reflect the property change of bridge components over time. In the present design, hinge joints are relatively weak compared to the beams; the cracking and deterioration of hinge joints would significantly change the load distribution among beams and thus change the system behavior of the bridge. Based on the observed condition of the Lake View Drive hinge joints and the general inability to assess the soundness in an inspection, it is recommended that the distribution factors should not be calculated in the traditional manner if it cannot be shown that the hinge joints are sound and able to transmit forces between beams [10]. Although consensus has been reached on the importance of strengthening the lateral connection between beams, no research has been conducted on how the lateral connection changes with time and how the bridge system behavior changes with the deterioration of the hinge joints. This paper presents a system performance evaluation approach for the precast adjacent concrete box beam bridges. A destructive test on a model bridge was conducted, and complementary 3D nonlinear finite element models were developed to demonstrate the performance change of the bridge over the complete loading cycle. The system performance analysis provides a basis for optimal new designs and rehabilitation strategies of this type of bridges.

2. Bridge System Performance Evaluation Approach

System safety was introduced to structural engineering domain after the collapse of the Ronan Point apartment building in London in 1968; structural redundancy and robustness are regarded as the indicators of structural system safety. In the last 30 years, attempts to measure structural redundancy and robustness have been made by researchers [11]. For the bridge system evaluation, methods proposed by Frangopol and Curley [12, 13] and Ghosn and Moses [14–16] have been adopted by the bridge standards and codes in America. In a first attempt to apply redundancy criteria in the bridge design specifications, the AASHTO LRFD Bridge Design Specifications [4] introduced a load modifier to the design check equation to account for redundancy based on the recommendation of Zhu [17]. Specifically, three load modifier values are recommended according to the redundancy classification of a member: 1.05 for nonredundant members, 1.0 for conventional level of redundancy, and 0.95 for exceptional level of redundancy. However, the specifications do not explain how to identify the redundancy levels of highway bridges; as explained in the LRFD Commentary, the recommended values have been subjectively assigned pending further research.

Zhu [17] proposed a redundancy factor that considers system type, correlation among the resistances of components, number of components in the system, and postfailure material behavior of components. The redundancy factor η_R is defined as the ratio of the mean resistance of a system, when its reliability index is 3.5, to the mean resistance of the off-system critical component. The main deficiency of this procedure is that idealized systems were used in developing the framework. In addition, the description of a structural system by use of series or parallel systems is a rather complex approach to system analysis, especially when nonlinear behavior is to be taken into account. Very few bridge engineers have the knowledge to perform a proper reliability analysis of a structure, which would hinder the acceptance and application of this approach. Therefore, there is room for further improvement in this procedure to fulfill the codification purpose.

Ghosn et al. [14–16] developed a set of quantitative measures of redundancy and robustness for highway bridges in terms of the capacity of the system, represented by LF_u, LF_f, and LF_d in Figure 2, as compared to the capacity of the weakest component, denoted by LF_1 in Figure 2, where LF_1 is considered the design strength of the bridge. Specifically, the three measures are defined as follows:

$$R_u = \frac{LF_u}{LF_1},$$

$$R_f = \frac{LF_f}{LF_1}, \tag{1}$$

$$R_d = \frac{LF_d}{LF_1},$$

(a) (b)

Figure 1: The collapse of exterior beams of adjacent concrete box beam bridges. (a) Lake View Drive Bridge, USA, 2005. (b) Third Hangzhou Qiantang Bridge, China, 2010.

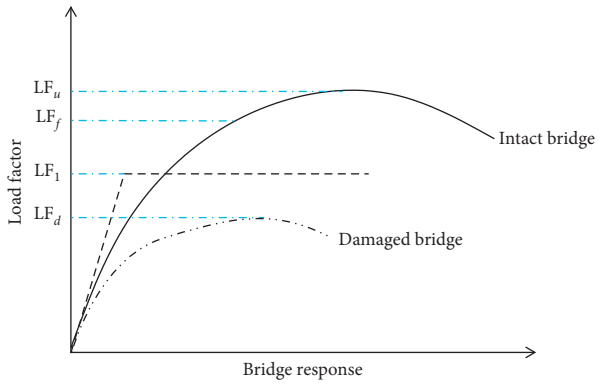

Figure 2: Representation of typical behavior of a bridge system [16].

where LF_u is the load that causes the failure of an originally intact bridge system; LF_f is the load that renders an originally intact bridge system exceeding functionality limit; LF_d is the load that causes the failure of a damaged system; R_u is the redundancy factor of an originally intact structure associated with the ultimate limit state; R_f is the redundancy factor of an originally intact structure associated with the functionality limit state; and R_d is the redundancy factor of a damaged structure, also called the robustness factor.

This procedure has been applied in the design of new bridges [18] and been incorporated in structural codes [19, 20]. The approach has also been adopted by [21] in developing a framework to include redundancy in the evaluation of existing railway bridges. The popular application of this procedure is partly attributed to the straightforward concept associated with its methodology. It models the structure directly as a system in a nonlinear analysis and evaluates the failure modes directly without analyzing the complex series and parallel system formulation.

The quantification of redundancy and robustness has been formulated in current bridge standards and codes, such as the system factors adopted in the AASHTO Manual of Bridge Evaluation 2018 [19]. However, no study has been made on the system reliability analysis for adjacent precast concrete box beam bridges. In addition, research associated with the redundancy and robustness of a bridge system mainly depends on simulation analyses; laboratory studies or real bridge verifications are rarely applied. Besides, in the simulation analysis of structural robustness, the sudden removal of a main member or connection is normally assumed, which does not include the situation of a member damage caused by degradation of the components or connections.

This paper investigates the system performance of adjacent precast concrete box beam bridges over a complete load range through a series of laboratory tests and 3D simulations. The objectives of the paper are to develop a framework to quantify the redundancy and robustness measurement of adjacent precast concrete beam bridges, and to experimentally verify the methodology adopted by the current Manual of Bridge Evaluation based on the National Cooperative Highway Research Program (NCHRP) reports 406, 458, and 776.

3. Load Transfer Mechanism of Adjacent Precast Concrete Box Beam Bridges

NCHRP Synthesis 393 summarized the connection details of adjacent precast concrete box beam bridges in America [22]. The adjacent box beams are generally connected by grouting in a longitudinal keyway between the beams, usually with transverse ties. Partial-depth or full-depth keyways are typically used, which are grouted by concrete of various mixes, epoxy grout materials, or high performance or even ultra-high performance concrete [23]. Transverse ties, grouted or ungrouted, are sometimes used. The ties may consist of a limited number of threaded reinforced rods, or

high-strength tendons posttensioned in multiple stages. The box beams may be covered with a concrete deck, forming a composite structure, or may not be.

For a typical superstructure of an adjacent concrete box beam bridge, parallel adjacent beams are tied together through hinge joints (or called shear keys), and the hinge joints are assumed to only bear shear but not transverse moment. When a load is applied on one or two beams, a portion of the load would be carried by the loaded beams, and the rest of the load is transferred to adjacent beams through hinge joints. The transverse moments are mostly countered through torsional stiffness of the beams. Hinge joints would also contribute a small portion of the transverse flexural stiffness of the bridge, but it is often neglected [24]. It is noted that bridge design codes, including national Chinese code JTG D-62 and AASHTO LRFD bridge design code, define the detail of hinge joints, while not requiring any calculation checks; thus empirical relations form the basis for some design guidelines. The lack of available analyses and models for the design of the connection between precast members represents an important issue in the construction of these systems [25].

Traffic or environment loads are transferred to adjacent beams via three mechanisms: (1) shear key configuration, (2) normal and shear stresses transferred at the interface between concrete components, and (3) shear reinforcement bar action [19].

The deflection of the i^{th} beam (denoted by $\omega_i(x)$) is proportional to the load (denoted by $P_i(x)$) or load effect acting on the beam (bending moment denoted by $m_i(x)$, shear force denoted by $g_i(x)$) or transferred to it, as shown in Figure 3; that is,

$$\frac{\omega_1(x)}{\omega_2(x)} = \frac{m_1(x)}{m_2(x)} = \frac{g_1(x)}{g_2(x)} = \frac{P_1(x)}{P_2(x)}. \tag{2}$$

4. Experimental Investigation

A model bridge with a scale of 1 : 2 (half size) was built based on the prototype design drawings for 10-meter adjacent box beam bridges in China. The model bridge consisted of four 5-meter long reinforced concrete beams that were designed so that their stresses were equivalent to those of a full scale beam. The model beam was designed complying with a Chinese code [26], and the calculation is included in the appendix. The dimensions of the prototype and model beam are summarized in Table 1. The compressive strength of concrete was 51.85 MPa, and the yield strength and the ultimate strength of reinforcement were 450 MPa and 580 MPa, respectively. The live-load distribution factor of the exterior beam was 0.4, which was calculated according to the design code.

The cross sections of the prototype and model beams are compared in Figure 4. Four φ16 reinforcement bars ($As = 804\ mm^2$) were used in the model beam section, with a 30 mm concrete cover. The amount of reinforcement was reduced from the original section so that its stresses were equivalent to those of a full scale beam. The crack load, yield load, and ultimate load of the model beam are 20.5 kN, 74.4 kN, and 86 kN, respectively.

The cross section of the model bridge is shown in Figure 5. Four beams were placed side by side and connected with cast-in-place concrete (some portion of the hinge joint concrete was sawn in previous nondestructive experiment and had been repaired using epoxy grout prior to this experimental study discussed herein) in the longitudinal joints. The beams and joints were covered with a plain concrete deck. No lateral tie rod was used. A composite action was formed between the beam and the concrete deck.

As shown in Figure 6, a stepwise concentrated load was placed at the midspan of beam #1 of the model bridge, and the load response of the loaded beam was shown in Figure 7. When the load reached 147 kN, it was automatically released, triggered by a sudden increase of the deflection, and the beam was reloaded to approximately the same applied load two more times; this is denoted by Load Case 1. In Load Case 2, a stepwise concentrated load was again applied at the midspan of beam #1, a "popping" was heard at an applied load of 131 kN, and the load was automatically dropped to 102 kN. After the completion of the above two loading cases, in Load Case 3, beam 4 was cut away from the bridge model along the joint (the deck on the beam was kept) and loaded until it yielded, existing cracks propagated visibly, and a "popping" was heard at an applied load of 89.5 kN; then the load was released and the beam was reloaded to approximately the same applied load two more times. The single beam was loaded in comparison with the beam behavior in the bridge system. It was observed that the bridge system kept some resistance after the loaded beam failed (the load reading reduced from 131 kN to 102 kN), but no resistance remained for the single beam (the load reading quickly returned to 0) after the failure of the loaded beam.

In Loading Cases 1 and 2, the relative vertical displacements between adjacent beams were monitored at three locations (girder end, midspan, $L/4$, and $3L/4$), as shown in Figure 8, the layout of the deflection gages. The change of the relative vertical displacements with load between beams #1 and #2 is demonstrated in Figure 7. A solid line of relative displacement of 0.0254 mm is added in the figure as a reference line. According to the research project performed by Case Western Reserve University for Ohio Department of Transportation, the relative displacement between adjacent beams should not exceed 0.001" (0.0254 mm) if the hinge joint is fully intact [6]. As shown in Figure 9, damage occurred at the early stage of loading because the relative deformation between beams 1 and 2 passed the 0.0254 mm line under a load less than 50 kN, while the design load of the beam is 86 kN. Thus, with a concentrated load placed at the midspan of beam #1 of the model bridge, the bridge failed in a sequence shown in Figure 10.

5. Finite Element Analysis

The experimental results were used to calibrate 3D nonlinear finite element (FE) models developed using Abaqus/CAE 6.14 software. The FE models were then utilized to predict

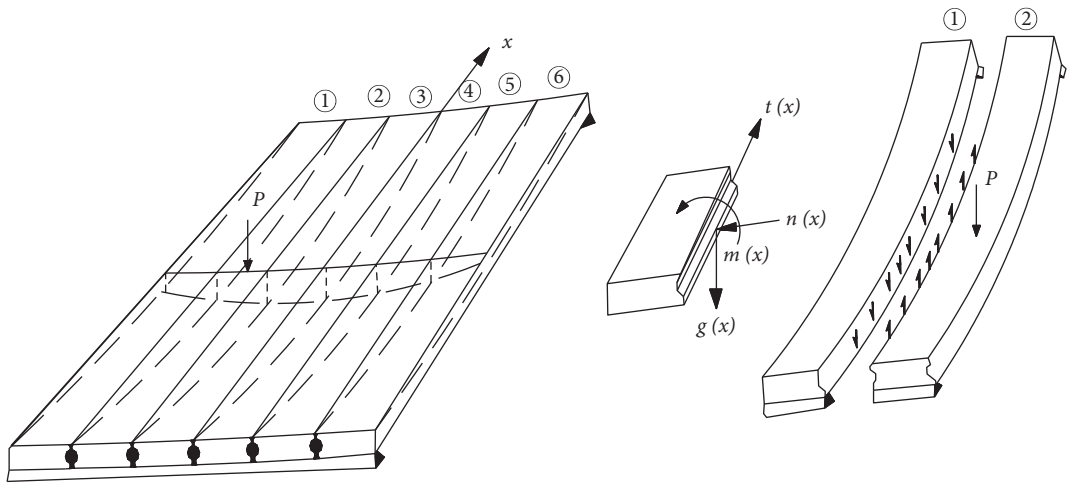

Figure 3: Stress diagram of adjacent beam bridges.

Table 1: Dimensions of a design prototype and a model bridge beam.

Items	Length of beam (cm)	Width of beam (cm)	Height of beam (cm)	Depth of hinge joint (cm)	Thickness of deck (cm)
Prototype	996	99	60	14	10
Test model	498	23	30	8.4	5

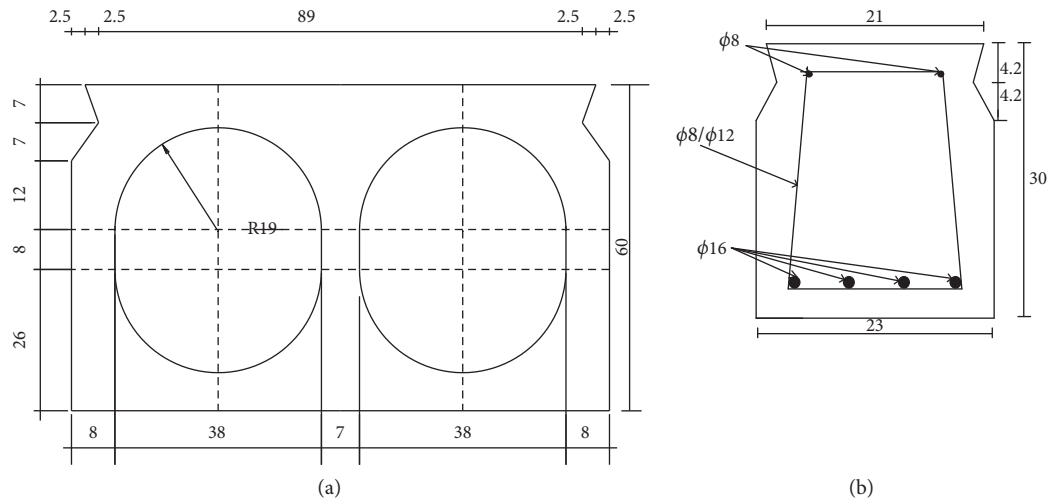

Figure 4: Cross section of the prototype and model beam (unit: cm). (a) Prototype beam cross section. (b) Model beam cross section.

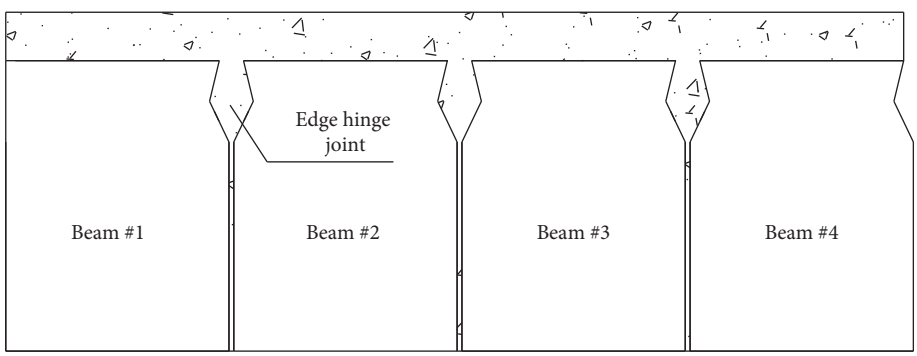

Figure 5: Cross section sketch of the model bridge.

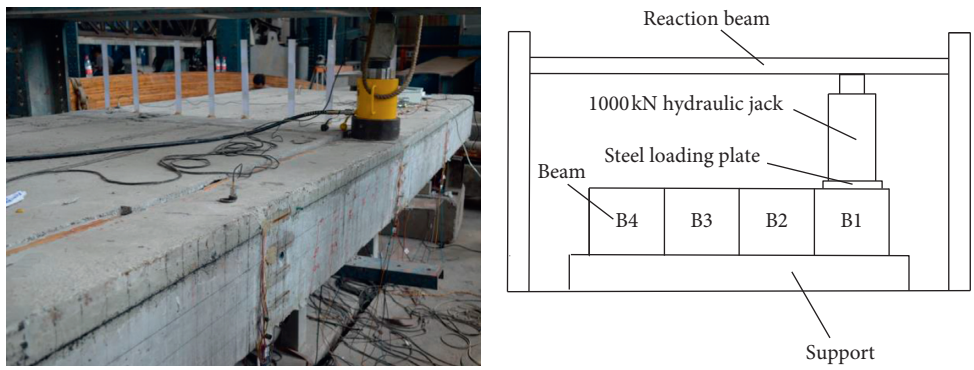

Figure 6: View of loading layout for the destructive test on the model bridge (the edge joint has cracked over loading). (a) Loading layout. (b) Elevation view.

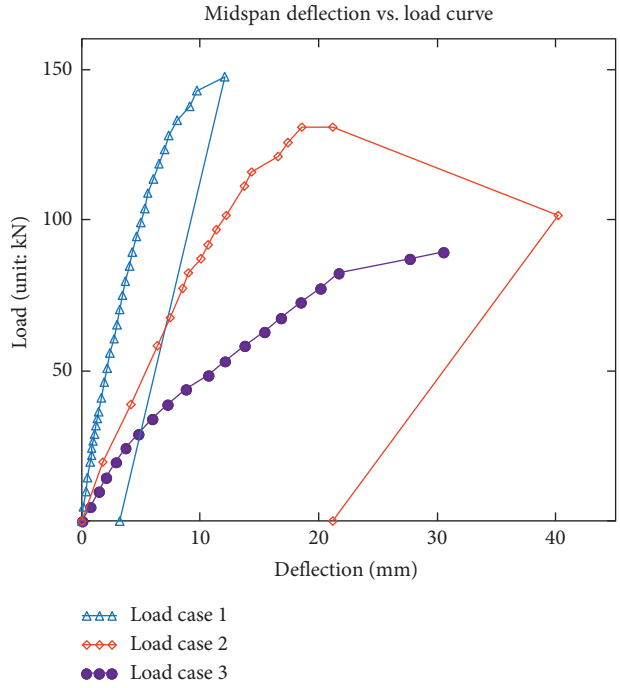

Figure 7: Response of the loaded beam.

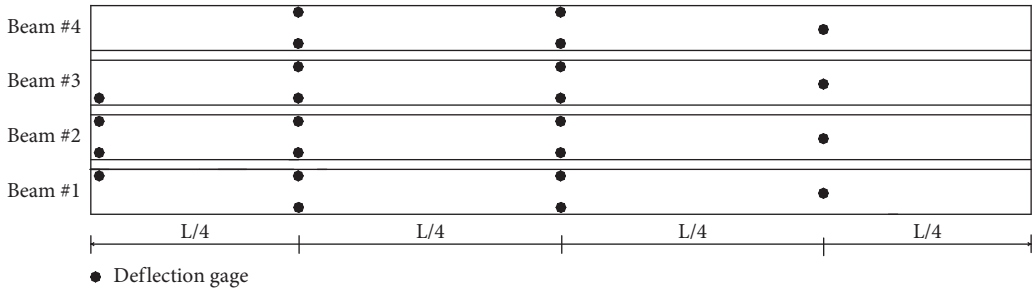

Figure 8: Layout of the deflection gages in Loading Cases 1 and 2.

the ultimate load capacity of the isolated simple beam and the model bridge, respectively.

The FE simulation agrees well with the experiment results, as shown in Figure 11. The calibrated FE model was extended to forecast the ultimate load of the beam, which was not obtained in the test because of the limitation of the instrument capability. Considering that the bridge structure was designed and constructed according to the Chinese

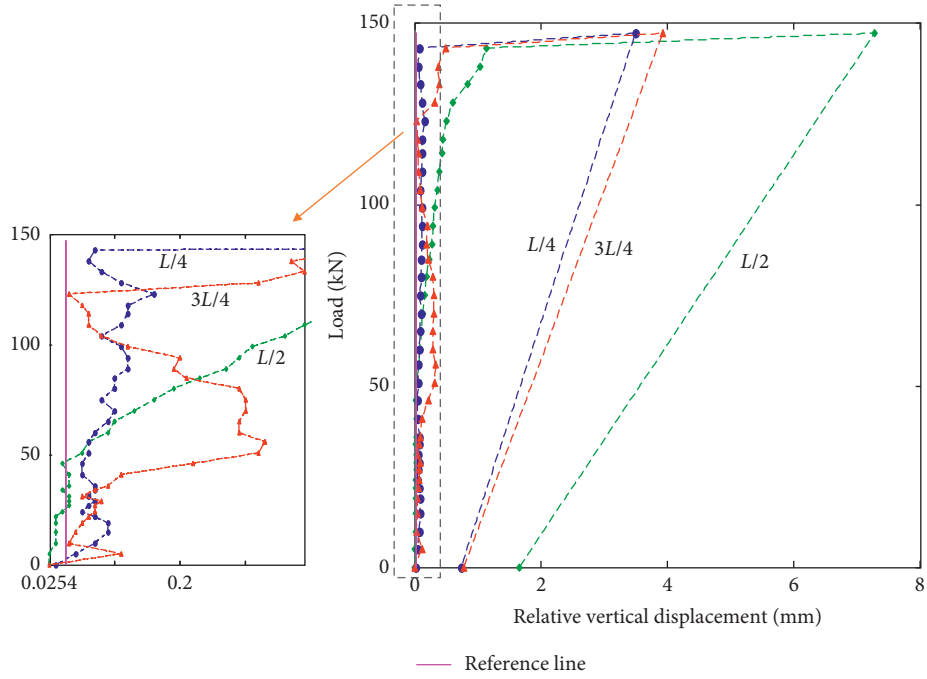

Figure 9: Relative vertical displacement at the edges of the two beams adjoining hinge joint #1.

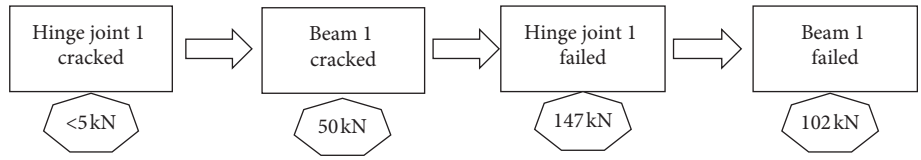

Figure 10: The failure sequence of model bridge in Load Case 1 and Load Case 2.

design code [26], the Chinese code criteria are considered herein. The Chinese code stipulated that the ultimate tensile strain of steel reinforcement bars is 0.01; the corresponding point load is 94.5 kN from the FE simulation. The yield strain of steel is 380 MPa/200,000, MPa = 0.002, and the corresponding point load is 79.5 kN. Moreover, the ultimate compressive strain of concrete is 0.0033, and the corresponding point load is 92 kN. From the serviceability point of view, a maximum displacement or an allowable hinge rotation usually serves as functionality criterion. A generally accepted functionality criterion is that the total live-load displacement should not be larger than $L/100$, where L is the span length [14]. From the FE model, the load that causes a midspan deflection of $L/100$ (47.3 mm) is 95 kN. Table 2 summarizes the above benchmarks.

The predicted failure mode of the model bridge is presented in Figure 12, which agrees well with the experimental results. Under a concentrated load placed at the midspan of beam #1, the severe cracking of hinge joint #1 triggers the "Single Plate Load Effect" and eventually causes the fracture of beam #1.

The deflection response of beam #1 to loading Case 1 is simulated and shown in Figure 13. It is observed that the simulation agrees well with the test results. The response beyond the yielding of beam #1 is also simulated over the full load range. TheThe limit of deflection is $L/100$, and the corresponding live load is deemed the maximum load. In particular, a live load of 144.8 kN caused a deflection of $L/100$ (47.3 mm), which is approximate to the magnitude of the theoretical fracture load (145 kN) of the main reinforcement predicted by simulation.

6. Change of Lateral Load Distribution Factor (LLDF) over the Full Load Range

Load distributed to each beam is proportional to the deflection or strain of the beam if the beams are identical and in the elastic range. Lateral load distribution factors (LLDF) are calculated according to this principle. No research has been performed to address the LLDF in the inelastic and plastic range up to date.

A deflection distribution factor (DDF), η, is put forward for the inelastic analysis as a substitution of LLDF.

$$\eta_i = \frac{w_i}{\sum_1^n w_i}, \tag{3}$$

where w_i is the deflection of the ith beam under vertical load obtained through load test or simulation.

The deflection of the ith beam of an adjacent box beam bridge can be expressed as

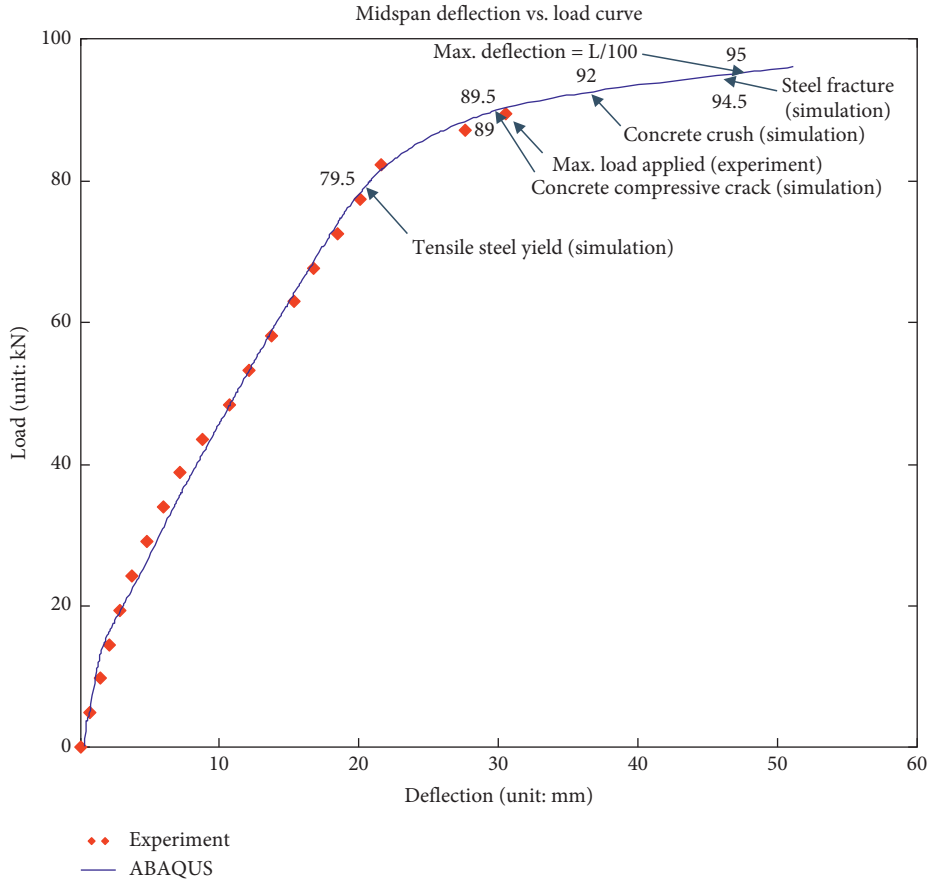

Figure 11: Response of a simple beam subjected to a point load.

Table 2: Benchmarks of a simple beam.

Benchmarks	Criteria	Corresponding load level obtained from simulation
Steel tensile yield strength	Tensile strain = 0.002	79.5 kN
Steel ultimate tensile strength (Chinese code)	Tensile strain = 0.01	94.5 kN
Concrete ultimate compressive strength	Compressive strain = 0.0033	92 kN
Concrete compressive crack strength	Compressive strain = 0.0016	89 kN
Maximum displacement level	Midspan deflection = $L/100$ = 47.3 mm	95 kN

$$w_i = \frac{P_i f(L)}{(EI)_i}, \tag{4}$$

where P_i is the load shared by the ith beam, $(EI)_i$ is the flexural stiffness of the ith beam, and L is the span length.

The flexural stiffness of a beam (EI) is not stable beyond the elastic range, which makes it impractical to use LLDF in the system performance analysis of the bridge. Fortunately the inelastic phase is not significant for the reinforced concrete structure, as shown in Figure 7. The deflection distribution factor is proposed accordingly to substitute the load distribution factor in the inelastic analysis. In Load Case 3 the simple beam experienced linear or near linear behavior until the load reached 79.5 kN, while in Load Case 1, the loaded beam (beam #1) demonstrated elastic behavior until the load reached 147 kN with η of 0.54, and the load shared by beam #1 is approximately 147 kN $*$ 0.54 = 79.4 kN. Similarly, the elastic load range is about 121 kN $*$ 0.66 = 79.9 kN.

The change of deflection distribution factor among beams with load is closely related to the robustness of adjacent precast box beam bridges. As shown in Figure 14, beam #1 was first in the linear range with a DDF of about 0.30 in Loading Case 1. The DDF increased slowly to about 0.37 when the point load on beam #1 reached 143 kN, and then jumped to 0.54 when beam #1 yielded. When the beam was reloaded in Loading Case 2, the DDF of beam #1 was about 0.57. The DDF soon increased to and stayed at about 0.6 until the load reached 92 kN, increased to 0.7 at 131 kN, then increased quickly to 0.84 when the beam collapsed, and the load then dropped to 102 kN. The process is summarized in Table 3.

The change of DDF reflects the condition deterioration of the hinge joints. The DDF of beam #1 was under 0.4 before

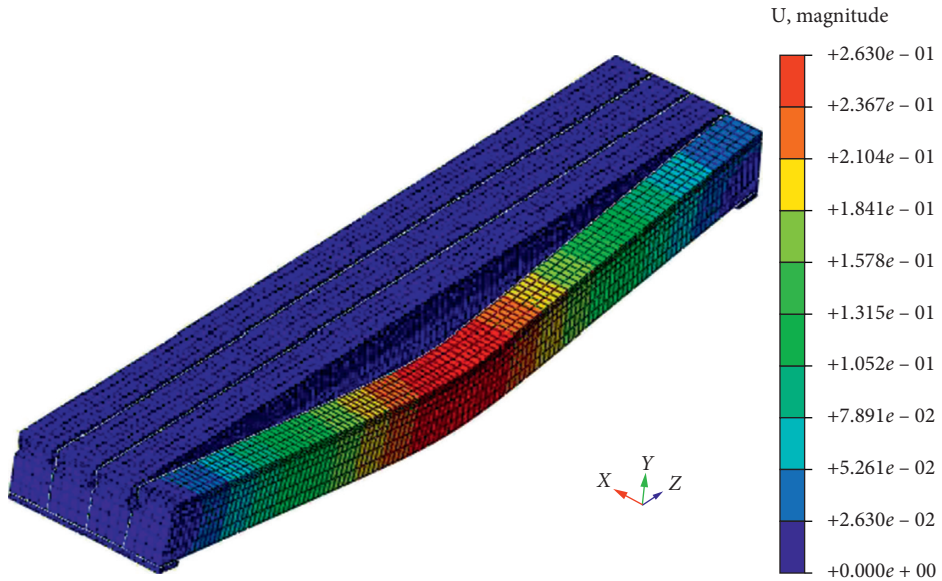

Figure 12: Failure mode of the model bridge under a concentrated load.

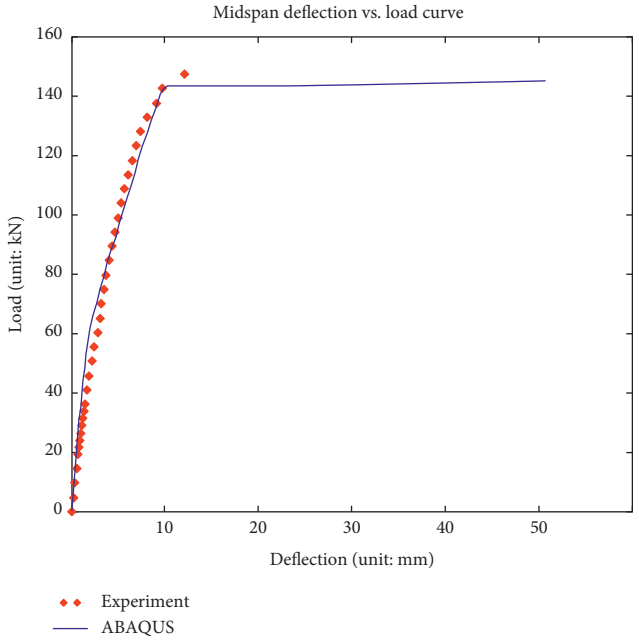

Figure 13: Response of the exterior beam of the model bridge subjected to a concentrated load.

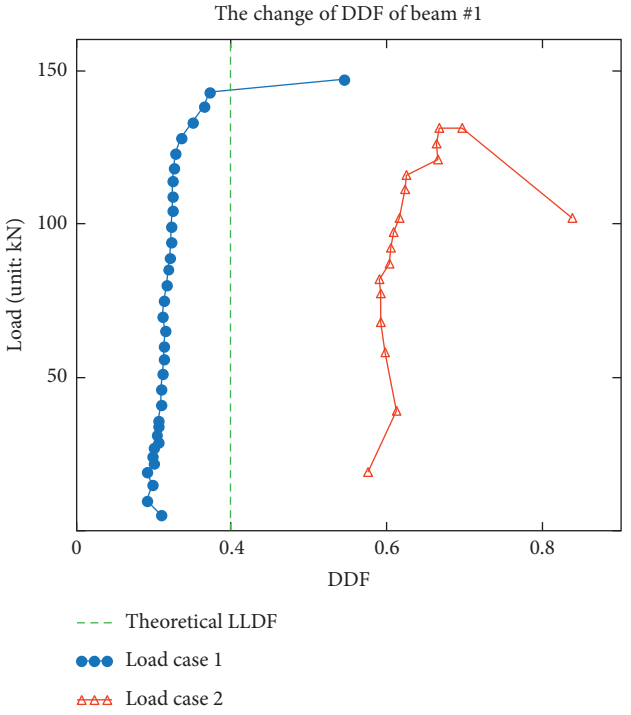

Figure 14: Change of deflection distribution factor with load.

hinge joint #1 lost its function, which verifies that the design load distribution factor value 0.4 is reasonable. In the evaluation of bridges in service, however, the change of DDF must be considered with the deterioration of the hinge joints.

In summary, the load transferring capacity to adjacent beams reduces with the deterioration of the hinge joints. When a hinge joint cracks, the crack path is irregular and the cracked hinge joint can still transfer loads. The hinge joint will gradually loose its function under cyclic loading and the continual leakage and corrosion. The change of the hinge joint condition will result in the change of load transfer among the adjacent beams. Note that hinge joints are secondary members in a bridge system; the influence of the damage of the hinge joints on the load capacity of the bridge has been overlooked. If the hinge joints are in sound condition, the distribution factors may be calculated in the traditional manner, However, when the hinge joints are (or suspected to be) in a severe condition, the actual load distribution factor may be significantly higher than the design values; thus, it is recommended that the influence of the hinge joints on the robustness of bridge systems is assessed.

Table 3: Change of DDF at different load stages.

Original condition	State	Concentrated load (kN)	Load distribution factor of beam #1
Intact bridge	Linear range	0~50	About 0.30
	Near linear range	50~118	0.30~0.32
	Maximum load applied	147	0.54
Damaged bridge	Ultimate capacity	131	0.70
	"Single Plate Load Effect" appeared	102	0.84

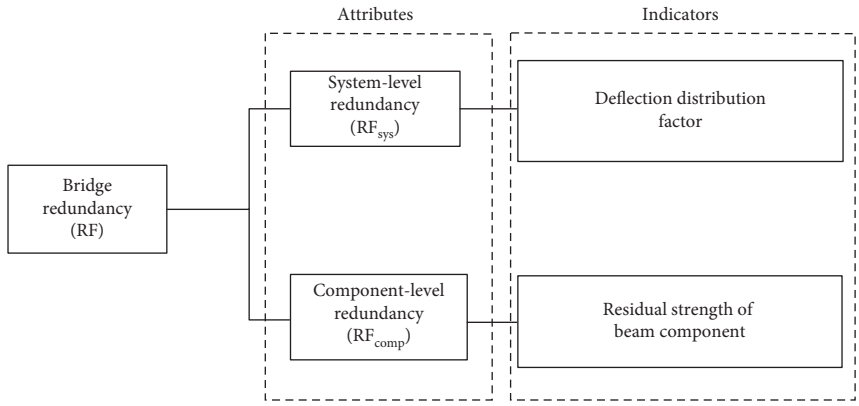

Figure 15: Redundancy and robustness of an adjacent box beam bridge.

7. Proposed Framework for Assessing Bridge Redundancy and Robustness

The authors propose to define redundancy for adjacent precast concrete beam bridges as the capacity of an originally intact bridge system to resist a load effect beyond the design load capacity of the bridge based on the critical member, and robustness as the load carrying capacity of a bridge system with damaged hinge joints. Redundancy could be used as an umbrella term for both redundancy and robustness under this definition [14, 16].

The load carrying capacity of an adjacent precast concrete beam bridge is presently evaluated by calculating the load distribution factors among the beams of the bridge and the ultimate section capacity of the beams. The total redundancy consists of two levels of redundancy: component and system level, as demonstrated in Figure 15. Material ductility and internal structural design of the components (e.g., number and layout of reinforcements) permit local yielding and redistribution of component internal forces (especially in most heavily loaded members), which is considered the component-level redundancy. Similarly, the load redistribution capacity among beams is considered the system-level redundancy. Studying both the component-level and system-level redundancy provides a full understanding of the mechanism of redundancy in a bridge system.

Both bridge redundancy and robustness are measured with rating factors (RF); the redundancy is calculated for intact bridges, denoted by RF_u, while robustness is for bridges with a major local damage, denoted by RF_d.

$$RF = RF_{\text{sys}} * RF_{\text{comp}},$$

$$RF_{\text{sys}} = \frac{\text{design load distribution factor}}{\text{measured deflection distributionn ratio}, \eta},$$

$$RF_{\text{comp}} = \frac{\text{measured Load Capacity of off} - \text{system beam}}{\text{design Load Capacity of off} - \text{system beam}}. \quad (5)$$

For the off-system beam (from the test of beam 4), $RF_{\text{comp}} = 89.5\,\text{kN}/88.6\,\text{kN} = 1.01$. For the originally intact model bridge, $RF_{\text{sys}} = (0.4/0.54) = 0.74$. Thus the redundancy factor of the originally intact bridge $RF_u = 0.75$.

For the damaged bridge model at ultimate state, $RF_{\text{sys}} = (0.4/0.70) = 0.57$, and the corresponding robustness factor $RF_{d1} = 0.56$.

When the Single Plate Load Effect occurs, the load distribution factor of beam #1 increased to 0.84; thus, $RF_{\text{sys}} = 0.4/0.84 = 0.48$, and the corresponding robustness factor $RF_{d2} = 0.48$.

For reinforced concrete beams, RF_{comp} is normally a little higher than 1.0 and can be neglected, and the design load distribution factor can be calculated with the method provided in a design code or through a linear analysis. The "measured (actual) deflection distribution factor" can be estimated through a finite element analysis based on the field hinge joint condition.

The present approaches for assessing bridge redundancy are mainly based on nonlinear finite element (FE) analyses. Unfortunately, the real behavior of bridges in the nonlinear range is difficult to evaluate, and a sound basis for the

nonlinear FE analysis is not available. In addition, a nonlinear FE analysis is not feasible for practitioners to use, while the computing complexity is reduced in the proposed method, which makes it suitable for the practitioners to use.

8. Redundancy Factors Using the Approach Proposed by NCHRP 406/776

The redundancy factors are calculated according to the approach proposed by Ghosn et al. [14–16] in NCHRP 406/776 and compared with the method proposed in this research. According to Ghosn et al., the load factor at the design strength is

$$LF_1 = \frac{R - M_D}{DF_1 M_L} = \frac{104.8 - 5.77}{0.4 \times 23.18} = 10.68, \quad (6)$$

where R is the ultimate load capacity of an off-system beam, which was theoretically predicted as 104.8 kN·m, corresponding to a midspan concentrated load of 88.6 kN as calculated according to the American Concrete Institute method [27]; M_D (5.77 kN·m) is the midspan moment caused by the dead load [3]; DF_1 is the load distribution factor for the exterior beam that is calculated as 0.40 according to the "hinge beam method" [28]; and M_L is the midspan moment caused by the design vehicle load of the prototype bridge, which was equivalent to a concentrated load of 18.62 kN placed at the midspan of the exterior beam (beam #1) that produces a positive moment of 23.18 kN·m [3].

The ultimate load capacity of the bridge system is obtained from the test as 145 kN; thus, $LF_u = 145\,\text{kN}/18.62\,\text{kN} = 7.79$, that is, the ratio of the ultimate load capacity over the design live load. Similarly, $LF_{d1} = 130\,\text{kN}/18.62\,\text{kN} = 6.98$ and $LF_{d2} = 100\,\text{kN}/18.62\,\text{kN} = 5.37$. The corresponding redundancy factors are

$$R_u = \frac{LF_u}{LF_1} = \frac{7.79}{10.68} = 0.73,$$

$$R_{d1} = \frac{LF_{d1}}{LF_1} = \frac{6.98}{10.68} = 0.65, \quad (7)$$

$$R_{d2} = \frac{LF_{d2}}{LF_1} = \frac{5.37}{10.68} = 0.50.$$

These factors are close to those calculated using the approach proposed in this research (0.75, 0.56, and 0.48). The threshold values for R_u and R_d defined in NCHRP reports 406, 458, and 776 are 1.30 and 0.50, respectively; thus, this bridge model does not provide adequate levels of redundancy and robustness.

9. Additional Points and Conclusions

The following conclusions are drawn from this research:

(1) If the hinge joints are in sound condition, the distribution factors may be calculated in the traditional manner as defined in design codes. However, when hinge joints are deteriorated and in a severe condition, the actual load distribution factors may be significantly higher than the design values. Considering the difficulty to assess the hinge joints in an inspection, the use of a more conservative load distribution factor or the employment of a reduced redundancy multiplier in the design of this type of bridges is recommended.

(2) System performance of a bridge varies with its structural conditions; for the model bridge, the redundancy factor is 0.73 for the originally intact system, 0.56 for the damaged system with a seriously cracked edge hinge joint, and 0.47 when the "Single Plate Load Effect" appears. Bridges with this type of hinge joints do not have adequate levels of redundancy and robustness.

(3) Deflection distribution factors can be used in the inelastic analysis for the system performance distribution of adjacent beam bridges. The new framework for redundancy rate calculation based on deflection distribution factors agrees well with the existing approaches with less computing complexity. The research outcome is based on one single load case, with the entire load applied on an edge girder. Modeling of more realistic loading scenarios for real bridges is on the schedule for future research to strengthen the approach proposed in this paper.

Appendix

The Design of the Model Beam

Midspan dead load moment of the prototype beam is

$$\text{M} = \frac{1}{8}ql^2 = \frac{1}{8} \times 24 \times (0.268856) \times 9.7 \times 9.7 = 75.89\,\text{kN·m}. \quad (A1)$$

Based on equivalent moment principle, a point load of 31.12 kN will cause a midspan moment of 75.89 kN·m.

$$Fc = 31.12\,\text{KN}. \quad (A2)$$

The equivalent coefficient for Fc is

$$C_p = C_L^2 C_E = \frac{1}{4}. \quad (A3)$$

The equivalent dead load moment on the model beam is $F_{H1} = Fc * C_\text{p} = 31.12/4 = 7.78$ kN.

The midspan dead load moment of the model beam is

$$M_1 = \frac{1}{8}ql^2 = \frac{1}{8} \times 24 \times (0.0671 + 0.0105) \times 4.98 \times 4.98 = 5.77\,kN \cdot m. \quad (A4)$$

Based on equivalent moment principle, a point load of 4.66 kN will cause a midspan moment of 5.77 kN·m.

$$F_{H1} = 4.64\,\text{KN}. \quad (A5)$$

Dead load difference is $F_2 = F_{H1} - F_{H2} = 7.78 - 4.46 = 3.32$ kN.

Midspan Vehicle Load Moment of the Prototype Beam

Midspan moment (vehicle impact is considered) is as follows: $M = (1+\mu)m\sum py_k$.

$$M = (1 + 0.05) * 0.2701 * (120 * 2.425 + 120 * 1.725 + 60 * 0.425) = 148.4672\,\text{kN} \times \text{m}. \quad \text{(A6)}$$

The equivalent midspan point load is

$$Fc = 30.6 * 2 = 61.2\,\text{KN}. \quad \text{(A7)}$$

The design moment at midspan is $Mu = 1.2M + 1.4M = 1.2 * 5.77 + 1.4 * 23.18 = 39.376$ kN·m.

For the model beam, the ultimate strength is as follows.

$$M_n = f_{cd}bx\left(h_0 - \frac{x}{2}\right) = 13.8 \times 230 \times 70.92\left(260 - \frac{70.92}{2}\right) = 50.54 \times 10^6\,\text{N·mm} = 50.54\,\text{KN·m} > \text{Mu}\,(= 39.376\,\text{KN·m}). \quad \text{(A8)}$$

Data Availability

The data used to support the findings of this study are available from the corresponding author upon request.

Conflicts of Interest

The authors declare that they have no conflicts of interest.

References

[1] H. G. Russell, "Adjacent precast concrete box-beam bridges: state of the practice," *PCI Journal*, vol. 56, no. 1, pp. 75–91, 2011.

[2] Y. Leng, J. Zhang, R. Jiang, H. He, and J. Zhou, "Experimental research on strengthening transverse connections of prefabricated concrete hollow core slab beam bridges," in *Proceedings of Paper presented at the Transportation Research Board 94th Annual Meeting*, Washington, DC, USA, January 2015.

[3] Y. Leng, "Study on crack behaviors of hinge joints for fabricated hollow slab bridges and transverse integrity reinforcement technology," Research Institute of Highway, MOT, Beijing, China, Master Dissertation, 2012.

[4] AASHTO, *AASHTO LRFD Bridge Design Specifications*, AASHTO (American Association of State Highway and Transportation Officials), Washington, DC, USA, 8th edition, 2017.

[5] JTG, *Code for Design of Highway Reinforced Concrete and Prestressed Concrete*, People's Communication Press, Beijing, China, 2004, in Chinese.

[6] A. Hucklebridge, H. El-Esnawl, and F. Mosses, "An investigation of load transfer in multi-beam prestressed box girder bridges," Report No. FHWA/OH-94-002, Deprtment of Civil Engineering, Case Western Reserve University, Cleveland, OH, USA, 1993.

[7] G. Annamalai and R. C. Brown, "Shear strength of post-tensioned grouted keyed connections," *PCI Journal*, vol. 35, no. 3, pp. 64–73, 1990.

[8] R. A. Miller, G. M. Hlavacs, T. Long, and A. Greuel, "Full-scale testing of shear keys for adjacent box girder bridges," *PCI Journal*, vol. 44, no. 6, p. 80, 1999.

[9] V. Perry and G. Weiss, "Innovative field cast UHPC joints for pre-cast bridge decks design, prototype testing and projects," in *Designing and Building with UHPFRC*, pp. 421–436, Wiley, Hoboken, NJ, USA, 2013.

[10] H. A. Kent, "Structural testing of prestressed concrete girders from the Lake view drive bridge," *Journal of Bridge Engineering*, vol. 14, no. 2, pp. 78–92, 2009.

[11] G. Anitori, J. R. Casas, and M. Ghosn, "Redundancy and robustness in the design and evaluation of bridges: European and North American perspectives," *Journal of Bridge Engineering*, vol. 18, no. 12, pp. 1241–1251, 2013.

[12] D. M. Frangopol and J. P. Curley, "Effects of damage and redundancy on structural reliability," *Journal of Structural Engineering*, vol. 113, no. 7, p. 17, 1987.

[13] N. M. Okasha and D. M. Frangopol, "Redundancy of structural systems with and without maintenance: an approach based on lifetime functions," *Reliability Engineering & System Safety*, vol. 95, no. 5, pp. 520–533, 2010.

[14] M. Ghosn and F. Moses, "Redundancy in highway bridge superstructures," NCHRP Report 406, University of Pittsburgh, Washington, DC, USA, 1998.

[15] W. D. Liu, M. Ghosn, F. Moses, and A. Neuenhoffer, "Redundancy in highway bridge substructures," NCHRP Rep. No. 458, Transportation Research Board, Washington, DC, USA, 2001.

[16] M. Ghosn and J. Yang, "Bridge system safety and redundancy," NCHRP Rep. No. 776, Transportation Research Board, Washington, DC, USA, 2014.

[17] B. Zhu, *Redundancy, reliability updating, and risk-based maintenance optimization of aging structures*, Ph.D thesis, Lehigh University, Bethlehem, PA, USA, 2015.

[18] F. Hubbard, T. Shkurti, and K. D. Price, "Marquette interchange reconstruction: HPS twin box girder ramps," 2004, http://www.structuremag.org/OldArchives/2004/october/SF-Marquette%20Interchange-October04-v2.pdf.

[19] AASHTO, *AASHTO Manual for Bridge Evaluation*, AASHTO MBE, Washington, DC, USA, 3rd edition, 2018.

[20] ISO, *Petroleum and Natural Gas Industries: Fixed Steel Offshore Structures*, ISO 19902, Geneva, Switzerland, 2007.

[21] D. Wisniewski, J. R. Casas, and M. Ghosn, "Load capacity evaluation of existing railway bridges based on robustness quantification," *Structural Engineering International*, vol. 16, no. 2, pp. 161–166, 2006.

[22] H. G. Russell, *Adjacent Precast Concrete Box Beam Bridges: Connection Details*, Transportation Research Board, Washington, DC, USA, 2009.

[23] H. Hussein, S. M. Sargand, F. T. A. Rikabi, and E. P. Steinberg, "Laboratory evaluation of ultrahigh-performance concrete shear key for prestressed adjacent precast concrete box girder bridges," *Journal of Bridge Engineering*, vol. 22, no. 2, Article ID 04016113, 2017.

[24] E. C. Hambly, *Bridge Deck Behaviour*, CRC Press, London, New York, 1991.

[25] D. M. Barbieri, Y. Chen, and E. Mazzarolo, "Longitudinal joint performance of a concrete hollow core slab bridge," *Transportation Research Record*, vol. 2672, no. 41, pp. 196–206, 2008.

[26] GB50010-2010, Code for Design of Concrete Structures, China, 2010, in Chinese.

[27] ACI, *Building Code Requirements for Structural Concrete and Commentary, ACI-318-19*, ACI (American Concrete Institute), Farmington Hills, MI, USA, 2019.
[28] L. S. Yao, *Bridge Engineering*, People's Transportation Publishing House, Beijing, China, 2008, in Chinese.